

# Berry Phase Effect on Exciton Transport and Bose Einstein Condensate

Wang Yao\* and Qian Niu

Department of Physics, The University of Texas, Austin, Texas 78712

(Dated: February 6, 2020)

We show a gauge structure that naturally exists for excitons in semiconductors. The resultant Berry phase effects on exciton center-of-mass motion are discussed for long-lived spatially indirect excitons in coupled quantum wells. Spin-dependent topological transport driven by mechanical and statistical forces are predicted. For trapped exciton gas, the Berry phase effect manifests as a spin-dependent revolving mechanism. When sufficiently large number of excitons have condensed, a nonrotating Bose-Einstein condensate may become unstable against vortex formation.

PACS numbers: 71.35.-y, 03.65.Vf, 73.43.-f, 03.75.Kk

Exciton in semiconductor is composed of a conduction band electron and a valence band hole bounded by Coulomb interaction, and its creation/annihilation absorbs/emits a photon. Due to the ultrashort recombination lifetime, excitons are mostly studied in the context of optics as source of nonlinear optical effects [1]. The realization of spatially indirect excitons by confining electrons and holes separately in two coupled quantum wells [2, 3] has substantially increased exciton lifetime up to  $\sim 10 \mu\text{s}$  [4], which opens up an entirely new realm of exciton dynamics. Transport phenomena of this metastable optical excitation is of interest. With the fundamental lengthscale limit for exciton transport being its Bohr radius  $a_B \sim 10 \text{ nm}$ , proper control to guide photo-created excitons from one spatial location to a different spatial location for photon emission [5, 6] may provide one possibility to beat the diffraction limit for light propagation. Moreover, recent experimental progresses on cold indirect exciton gases in coupled quantum wells suggest that exciton Bose-Einstein condensation as a new matter state of fundamental interest may become in reach after decades of its prediction [7, 8, 9, 10, 11, 12].

In this letter, we investigate an intrinsic gauge structure in the exciton wavefunction and its effect on exciton transport and Bose-Einstein condensation. In general, dynamics restricted in a subspace is subjected to a gauge field known as Berry curvature, which encodes information about the rest of Hilbert space projected away [13]. The exciton gauge structure explored here has two origins: (i) the electron and hole constitution restricted to certain Bloch bands; and (ii) the relative motion restricted to certain hydrogen-like orbit. We show that the resultant Berry curvature manifests on the exciton center-of-mass motion as a *momentum space* magnetic field conditioned on the exciton spin. This gives rise to spin-dependent topological transport of excitons driving by mechanical or statistical forces, similar to the topological transport of Bloch electrons arising from Berry curvatures in the Bloch band [14, 15, 16, 17]. The long radiative lifetime and long diffusion length of indirect excitons will allow observation of these effects from a spatial map of luminescence polarization, which may provide direct

evidence on Berry phase supported topological transport and may help to resolve the controversy on the importance of such an intrinsic contribution to the anomalous Hall effect and spin Hall effect. Moreover, in a trapping potential, we show novel consequences of the Berry curvature. This momentum-space gauge field tends to revolve trapped exciton gases with spin-dependent circular motion, and contributes a spin-dependent energy correction to vortex state in a Bose-Einstein condensate. We show that when sufficiently large number of excitons have condensed, a nonrotating condensate may become unstable against formation of vortex state.

*Gauge structure in exciton wavefunction.*—In a homogeneous system, the exciton energy-momentum eigenstate is parameterized by the center-of-mass wavevector  $\mathbf{q}$  and the quantum number  $n$  for each hydrogen-like orbit of the relative motion. The wavefunction can be generally written as  $\Psi_{n,\mathbf{q}}^{\text{ex}} = e^{i\mathbf{q}\cdot\mathbf{R}}U_{n,\mathbf{q}}^{\text{ex}}$  with  $\mathbf{R}$  being the center-of-mass coordinate. Like the Bloch function, the exciton wavefunction is decomposed into a plane-wave envelope function for center-of-mass motion and an ‘internal’ structure  $U_{n,\mathbf{q}}^{\text{ex}} = \sum_{\mathbf{k}} F_n(\mathbf{k}, \mathbf{q}) e^{i\mathbf{k}\cdot\mathbf{r}} u_{e,\mathbf{k}+\frac{m_e}{M}\mathbf{q}} u_{h,-\mathbf{k}+\frac{m_h}{M}\mathbf{q}}$  where  $\mathbf{k}$  and  $\mathbf{r}$  are respectively the wavevector and coordinate for the relative motion.  $u_{e,\mathbf{k}_e}$  and  $u_{h,\mathbf{k}_h}$  are the periodic part of the electron and hole Bloch function, and  $\sum_{\mathbf{k}} F_n(\mathbf{k}, \mathbf{q}) e^{i\mathbf{k}\cdot\mathbf{r}}$  gives the envelope function of the relative motion which may depend on  $\mathbf{q}$  in general.  $M \equiv m_e + m_h$  is the exciton mass. Similar to that of the Bloch electrons [15, 16], the gauge structure of exciton lies in the dependence of the ‘internal’ structure  $U_{n,\mathbf{q}}^{\text{ex}}$  on the dynamical parameter  $\mathbf{q}$  [13]. The gauge potential is defined as  $\mathcal{A}_\mu^{\text{ex}} \equiv i \langle U^{\text{ex}} | \partial_{q_\mu} | U^{\text{ex}} \rangle$ , and the gauge field is then  $\Omega^{\text{ex}} \equiv \nabla_{\mathbf{q}} \times \mathcal{A}^{\text{ex}}$ . This gauge field, known as the Berry curvature, is analogous to a ‘magnetic’ field in the crystal momentum space. Its integral over a  $q$ -space area yields the Berry phase of an exciton state adiabatically going around along the boundary of the area, which is similar to the relationship between a magnetic field and the Arharonov-Bohm phase.

For 2D exciton, the Berry curvature is always normal

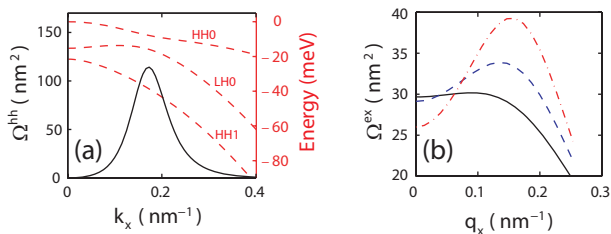


FIG. 1: Gauge structure in GaAs quantum well. (a) Dashed curves denote the dispersion relation of three highest valence subbands in a 10nm thick quantum well layer with valence barrier height of 140 meV. Berry curvature (solid curve) in heavy-hole subband HH0 is most pronounced at the in-plane wavevector where the HH0 subband anti-cross with the light-hole subband LH0. In the calculation, the same Luttinger parameters ( $\gamma_1 = 6.85$ ,  $\gamma_2 = 2.1$ , and  $\gamma_3 = 2.9$ ) is used for the quantum well layer and the barrier. (b) Berry curvature as a function of center-of-mass wavevector for 1s heavy-hole exciton. We assume the in-plane exciton Bohr radius  $a_B = 8, 10$ , and 12 nm for solid, dashed and dash-dotted curves respectively.

to the plane with magnitude given by,

$$\begin{aligned} \Omega^{ex}(\mathbf{q}) = & \left(\frac{m_h}{M}\right)^2 \sum_{\mathbf{k}} |F|^2 \Omega^h\left(-\mathbf{k} + \frac{m_h}{M}\mathbf{q}\right) \\ & + i \sum_{\mathbf{k}} (\partial_{q_x} F^* \partial_{q_y} F - \partial_{q_y} F^* \partial_{q_x} F) \\ & + \frac{m_h}{M} \sum_{\mathbf{k}} \left[ \partial_{q_x} |F|^2 \mathcal{A}_y^h\left(-\mathbf{k} + \frac{m_h}{M}\mathbf{q}\right) - x \leftrightarrow y \right] \end{aligned} \quad (1)$$

where  $\mathcal{A}_\mu^h(\mathbf{k}) \equiv i \langle u_{h,\mathbf{k}} | \partial_{k_\mu} | u_{h,\mathbf{k}} \rangle$  and  $\Omega^h(\mathbf{k}) \equiv \nabla_{\mathbf{k}} \times \mathcal{A}^h(\mathbf{k})$  are respectively the gauge potential and gauge field in the hole band. The Berry curvature of the exciton thus has three contributions: (i) inheritance of Berry curvatures from the Bloch bands to which the electron and hole constituents are restricted; (ii) entanglement of relative motion in  $n$ th orbit with the center-of-mass motion; (iii) cross terms of the two. Contribution from conduction band Berry curvature is neglected here due to its smallness and the further suppression by a prefactor  $\frac{m_e}{M} \ll 1$  when the hole effective mass is much heavier. In quantum well, heavy-hole light-hole mixing at finite in-plane wavevector leads to pronounced Berry curvature distributions in these subbands [18], and we expect this to be the dominant contribution to the exciton Berry curvature [Fig. (1)]. As  $\Omega^h$  depends on the hole spin, the exciton dynamics thus acquires a spin-dependent ingredient. More specifically, for 1s heavy-hole excitons being investigated for transport and condensation phenomena [4, 7, 8, 9, 10, 11, 12], the Berry curvature distribution is opposite between the two ‘bright’ exciton branches  $e_+^\dagger h_-^\dagger |G\rangle$  and  $e_-^\dagger h_+^\dagger |G\rangle$ , and between the two ‘dark’ exciton branches  $e_+^\dagger h_+^\dagger |G\rangle$  and  $e_-^\dagger h_-^\dagger |G\rangle$  [19]. This feature is also evident from the odd parity of  $\Omega^{ex}$  under time reversal operation.

*Semiclassical Equation of Motion.*—From now on, we focus on spatially indirect excitons with long radiative lifetime. To see the effect of Berry curvature, we first establish the semiclassical theory for wavepacket dynamics of excitons subject to perturbations varying slowly in space and time. Consider the following exciton wavepacket centered at center-of-mass coordinate  $\mathbf{R}_c$ :  $|X\rangle = \int [d\mathbf{q}] w(\mathbf{q}) |\Psi_{\mathbf{q}}^{ex}\rangle$ .  $w(\mathbf{q})$  is a function localized around  $\mathbf{q}_c$  with a width much smaller than the inverse of the in-plane exciton Bohr radius  $a_B$ , and  $\int [d\mathbf{q}]$  stands for  $\int d\mathbf{q} (2\pi)^{-2}$  here and hereafter. The equation of motion for this wavepacket can be derived from the effective Lagrangian [16],

$$\dot{\mathbf{R}}_c = \frac{\partial \mathcal{E}(\mathbf{q}_c, \mathbf{R}_c)}{\partial \mathbf{q}_c} - \dot{\mathbf{q}}_c \times \Omega^{ex}, \quad (2a)$$

$$\dot{\mathbf{q}}_c = -\frac{\partial \mathcal{E}(\mathbf{q}_c, \mathbf{R}_c)}{\partial \mathbf{R}_c} - \dot{\mathbf{R}}_c \times \mathcal{D}. \quad (2b)$$

where and hereafter we use the convention  $\hbar = 1$ .  $\mathcal{E}(\mathbf{q}_c, \mathbf{R}_c)$  is the semiclassical energy of the exciton wavepacket with center-of-mass wavevector  $\mathbf{q}_c$  and coordinate  $\mathbf{R}_c$ . To leading order, it is of a factorized form  $\mathcal{E}(\mathbf{q}_c, \mathbf{R}_c) \equiv \mathcal{E}_0(\mathbf{q}_c) + V(\mathbf{R}_c)$  where  $\mathcal{E}_0(\mathbf{q}_c)$  is the unperturbed exciton dispersion in the homogeneous QW and  $V$  is the potential energy from spatial dependent external perturbations. Hence, the exciton center-of-mass motion is subjected to a mechanical force  $\mathcal{C} \equiv -\nabla V$ . In an electrostatic potential  $\phi$ ,  $\mathcal{C}_{x,y} \equiv ed\partial_{x,y} \frac{\partial \phi}{\partial z}$  with  $d$  being the separation between the electron and hole layers [20]. Thus, the intrinsic dipole moment of indirect exciton allows its transport to be controlled by the electric field gradient, which forms the basis of electrically gated excitonic circuits [5, 6]. The dipole moment also allows a *real-space* ‘magnetic’ field  $\mathcal{D} \equiv ed \frac{\partial B_z(\mathbf{R}_c)}{\partial z} \hat{z}$  from the gradient of the external magnetic field  $\mathbf{B}(\mathbf{r})$ . In conjugation, the Berry curvature  $\Omega^{ex}$  indeed plays the role of a *momentum-space* ‘magnetic’ field which give rises to an anomalous contribution to the velocity [16].

*Spin Hall effect and Spin Nernst effect.*—The above semiclassical equation of motion is the basis for calculation of exciton transport currents driven by mechanical and statistical forces. The exciton current density can be defined as  $\mathbf{J} \equiv \int [d\mathbf{q}_c] f \dot{\mathbf{R}}_c$  where  $f = f(\mathbf{q}_c, \mathbf{R}_c)$  is the distribution function. In an electrically controlled excitonic circuit [5, 6], the flow of excitons is driven by the ‘electric-like’ force  $\mathcal{C}$  from patterned electrodes [20]. We immediately find that the anomalous velocity term in Eq. (2a) contributes a spin-dependent exciton Hall current:  $\mathbf{J}_H = \mathcal{C} \times \int [d\mathbf{q}_c] f(\mathbf{q}_c) \Omega^{ex}(\mathbf{q}_c)$ .

In most current experiments, hot indirect exciton gas are generated at laser excitation spot, and the exciton temperature decreases by phonon emissions upon diffusion to remote trap regions [7, 8, 9, 10, 11, 12]. ‘Thermoelectric’ responses to the statistical forces of temperature gradient and chemical potential gradient is thus

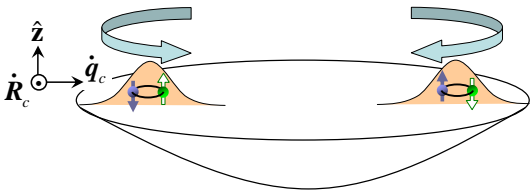


FIG. 2: Motion of indirect excitons in trap. The Berry curvature induces an anomalous velocity transverse to the force from the trap. The direction of the resultant circulation in center-of-mass motion depends on the exciton spin states.

of direct relevance. From the basis of the Einstein relation, it is suggested that an exciton spin Hall current can be induced by a chemical potential gradient. Furthermore, the Mott relation for the ‘electrical’ conductivity and ‘thermoelectric’ conductivity suggests the *spin Nernst effect*, i.e. spin Hall current driven by a temperature gradient. Both relations are proved to hold for Berry phase supported topological transport currents of Bloch electrons [17], and the conclusion is straightforwardly generalized to excitons of Boson statistics. Specifically, we find the spin-dependent exciton Hall current in the presence of chemical potential gradient and temperature gradient:  $\mathbf{J}_H = \nabla\mu \times \int [d\mathbf{q}_c] f \Omega^{\text{ex}} + \frac{\nabla T}{T} \times \int [d\mathbf{q}_c] \Omega^{\text{ex}} [(\mathcal{E} - \mu)f + k_B T \log(1 - e^{-\beta(\mathcal{E} - \mu)})]$ .

It is interesting to make a comparison with the spin Hall effect recently observed on exciton-polaritons [21], which results from the co-effect of disorder scattering and the ‘spin-orbit’ coupling (i.e. the momentum dependent polarization splitting) for spatially direct excitons. In contrast, for indirect excitons, the polarization splitting is negligible as the wavefunction overlap between the electron and hole component is small [22]. Therefore, the spin Hall and spin Nernst transport will be dominated by the *intrinsic* mechanism of Berry curvatures, which may be referred as *clean* contribution since no disorder scattering is required [14].

*Berry Phase Effect on Exciton Condensate.*—In 2D, Bose-Einstein condensation is possible only in a trap [23]. In a confining potential  $V(\mathbf{R})$ , the anomalous velocity from the Berry curvature results in a spin-dependent circulation motion for uncondensed excitons [Fig. 2]. To consider the Berry phase effect on condensed excitons in trap, we first establish the effective quantum Hamiltonian in presence of the Berry curvature. From Eq. (2), it is evident that, with finite  $\Omega^{\text{ex}}$ , the physical position and momentum of the exciton wavepacket no longer form a canonical pair. Quantization of the non-canonical equation of motion is possible by finding the canonical position and momentum variables  $\mathbf{R}$  and  $\mathbf{q}$  which are related to the physical ones by:  $\mathbf{R}_c = \mathbf{R} + \mathcal{A}(\mathbf{q}); \mathbf{q}_c = \mathbf{q}$  [24]. This is simply a generalization of the Peierls substitution to the momentum-space gauge field. The semiclassical energy of the exciton can then be expressed in

terms of the canonical position and momentum variable as  $\mathcal{E}(\mathbf{R}, \mathbf{q}) = \mathcal{E}_0(\mathbf{q}) + V(\mathbf{R}) + \nabla V \cdot \mathcal{A}(\mathbf{q})$ . Taking the standard quantization procedure, we obtain the modified Gross-Pitaevskii equation with the Berry phase effect

$$\left[ -\frac{\nabla^2}{2M} + V + U_0 |\Psi(\mathbf{R})|^2 + \nabla V \cdot \hat{\mathcal{A}} \right] \Psi(\mathbf{R}) = \mu \Psi(\mathbf{R}), \quad (3)$$

where  $\hat{\mathcal{A}} \equiv \mathcal{A}(-i\nabla)$  is an operator acting on the condensate wavefunction  $\Psi(\mathbf{R})$ .  $U_0 = e^2 d/\epsilon$  is the strength of the repulsive dipole-dipole interaction between indirect excitons [25]. The last term on the right hand side shows the Berry phase effect. In a harmonic trap  $V(\mathbf{R}) = \frac{1}{2} M \omega_c^2 R^2$  with characteristic length  $a_{\text{osc}} \equiv (M \omega_c)^{-1/2} \ll a_B$ , this term reduces to  $\nabla V \cdot \hat{\mathcal{A}} = M \omega_c^2 \Omega_0 \hat{L}_z$  where  $\Omega_0 \equiv \Omega^{\text{ex}}(\mathbf{q} = 0)$  and  $\hat{L}_z$  is the angular momentum operator.

In the multi-component exciton condensate, the Berry phase term is diagonal in the spin subspace while interconversion between different spin components is incoherent via the exciton spin relaxation processes [26]. We first analyze how the Berry curvature affect each component individually. Obviously, the Berry phase term will lead to a spin-dependent energy correction to the states with finite angular momentum. To create a vortex with a single quantized circulation, the cost of energy in absence of Berry curvature is:  $\varepsilon_v = \pi n_0 M^{-1} \ln(0.888 \frac{\rho}{\xi_0})$  [27], where  $n_0$  and  $\xi_0$  are respectively the exciton density and healing length at the trap center without vortex, and  $\rho$  is the spatial dimension of the exciton condensation which, in the Thomas-Fermi approximation, is given by  $\rho = a_{\text{osc}} (U_0 N M)^{1/4}$ . The Berry phase term contribute an energy correction  $\Delta \varepsilon_v = M \omega_c^2 \Omega_0 \mathcal{L}_v$  where  $\mathcal{L}_v = \pm \frac{1}{2} n_0 \pi \rho^2$  is the angular momentum of the vortex state [27]. When  $\Omega_0$  and  $\mathcal{L}_v$  have opposite sign, the Berry curvature reduces the energy cost of creating a vortex in the corresponding spin component of the condensate. Further, when  $\varepsilon_v + \Delta \varepsilon_v < 0$ , a nonrotating condensate component becomes unstable upon forming a vortex. As  $\mathcal{L}_v$  is quadratic while  $\varepsilon_v$  is logarithmic in the condensate size  $\rho$ , such instability occurs when the number of condensed excitons is larger than  $N_{\text{vor}} \sim (U_0 M^3 \omega_c^2 \Omega_0^2)^{-1}$ .

With the increase of density, the excitonic condensate will cross from BEC of tightly bound excitons to BCS type momentum-space  $e$ - $h$  pairing [22, 28]. In the harmonic trap, the border size for such crossover is roughly  $N_c \sim (U_0^{-1} M \omega_c^2 a_B^4)^{-1}$ , corresponding to the density  $\sim a_B^{-2}$ . Thus, for sufficiently large  $U_0 M$ ,  $N_{\text{vor}} \ll N_c$  and the instability is reached well in the BEC end where the above treatment of condensate is valid. In typical GaAs coupled quantum well systems, our calculations show that spontaneous vortex formation in BEC phase is expected only in tight confinement which may be realized in electrostatic traps (see Fig. 3) [20].

*Conclusions and Outlooks.*—We have discussed a gauge structure that naturally exists in exciton wavefunc-

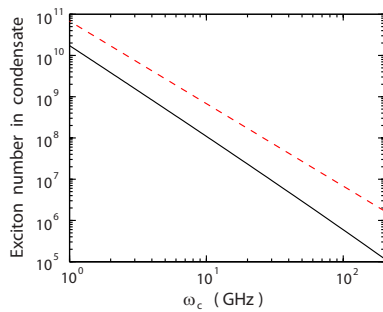


FIG. 3: Critical condensate size as a function of harmonic trap frequency  $\omega_c$ .  $N_{\text{vor}}$  is shown by solid curve above which the condensate is unstable against vortex formation. Dashed curve denotes  $N_c$  for BEC-BCS crossover. We have assumed GaAs coupled quantum well where electron and hole layers are separated by  $d = 10$  nm, and the exciton Berry curvature is taken from the  $a_B = 10$  nm curve in Fig. 1(b).

tion and the resultant Berry phase effect on exciton dynamics. A direct consequence is the spin-dependent topological transport of excitons driven by mechanical and statistical force, which may add novel spin functionalities into excitonic circuits [5, 6]. Of particular interest is the coupling of the Berry curvature to the angular momentum of a trapped wavefunction which may lead to instability of nonrotating Bose-Einstein condensate above the critical size  $N_{\text{vor}}$ . As the tendency of forming vortex and anti-vortex depends on the spin species and the instability can be simultaneously reached in each spin component under equilibrium, an interesting problem of vortex formation dynamics is posed for future study. If the wavefunctions of different spin components are driven into different angular momentum states, exciton spin relaxation processes can lead to fast depletion of the condensate. Such dynamics may be experimentally probed from the angular distribution of photoluminescence [25]. In GaAs coupled quantum well with moderate trap,  $N_{\text{vor}}$  extrapolated from the BEC end analysis approaches the border size  $N_c$  for BEC-BCS crossover [Fig. 3]. Thus, proper treatment in the entire crossover regime is of interest, and we expect that Berry phase effect could be important in other phases of the excitonic condensate [28, 29]. Recently, observation of Bose-Einstein condensation have been reported on microcavity polaritons [30]. As polariton can inherit the gauge structure from its exciton portion, we expect Berry phase effect shall also manifest in polariton dynamics.

The work was supported by NSF, DOE, the Welch Foundation, and NSFC.

\* wangyao@physics.utexas.edu

[1] D. S. Chemla and J. Shah, Nature **411**, 549 (2001).

- [2] A. Alexandrou *et al.*, Phys. Rev. B **42**, 9225 (1990).  
 [3] L. V. Butov, A. Zrenner, G. Abstreiter, G. Böhm, and G. Weimann, Phys. Rev. Lett. **73**, 304 (1994).  
 [4] Z. Voros, R. Balili, D. W. Snoke, L. Pfeiffer, and K. West, Phys. Rev. Lett. **94**, 226401 (2005).  
 [5] D. W. Snoke, Photonics Spectra **40**, 108 (2006).  
 [6] A. A. High, A. T. Hammack, L. V. Butov, M. Hanson, and A. C. Gossard, Opt. Lett. **32**, 2466 (2007).  
 [7] L. Butov, C. W. Lai, A. L. Ivanov, A. C. Gossard, and D. S. Chemla, Nature **417**, 47 (2002).  
 [8] L. Butov, A. C. Gossard, and D. S. Chemla, Nature **418**, 751 (2002).  
 [9] D. Snoke, S. Denev, Y. Liu, L. Pfeiffer, and K. West, Nature **418**, 754 (2002).  
 [10] Z. Voros, D. W. Snoke, L. Pfeiffer, and K. West, Phys. Rev. Lett. **97**, 016803 (2006).  
 [11] S. Yang, A. T. Hammack, M. M. Fogler, L. V. Butov, and A. C. Gossard, Phys. Rev. Lett. **97**, 187402 (2006).  
 [12] S. Yang, A. V. Mintsev, A. T. Hammack, L. V. Butov, and A. C. Gossard, Phys. Rev. B **75**, 033311 (2007).  
 [13] M. V. Berry, Proc. R. Soc. London Ser. A **392**, 45 (1984).  
 [14] S. Murakami, N. Nagaosa, and S.-C. Zhang, Science **301**, 1348 (2003); J. Sinova *et al.*, Phys. Rev. Lett. **92**, 126603 (2004).  
 [15] D. J. Thouless, M. Kohmoto, M. P. Nightingale, and M. den Nijs, Phys. Rev. Lett. **49**, 405 (1982).  
 [16] M.-C. Chang and Q. Niu, Phys. Rev. B **53**, 7010 (1996).  
 [17] D. Xiao, Y. Yao, Z. Fang, and Q. Niu, Phys. Rev. Lett. **97**, 026603 (2006).  
 [18] W. Yao, A. H. MacDonald, and Q. Niu, Phys. Rev. Lett. **99**, 047401 (2007).  
 [19]  $e_{\pm}^{\dagger}$  denotes the creation operator for electron in the conduction subband with  $S_z = \pm \frac{1}{2}$ , and  $h_{\pm}^{\dagger}$  for hole in the heavy-hole subband HH0 arising from the  $J_z = \mp \frac{3}{2}$  band-edge state.  
 [20] A. T. Hammack *et al.*, J. Appl. Phys. **99**, 066104 (2006).  
 [21] A. Kavokin, G. Malpuech, and M. Glazov, Phys. Rev. Lett. **95**, 136601 (2005); C. Leyder *et al.*, Nature Physics **3**, 628 (2007); W. Langbein *et al.*, Phys. Rev. B **75**, 075323 (2007).  
 [22] P. B. Littlewood *et al.*, J. Phys.: Condens. Matter **16**, S3597 (2004).  
 [23] V. Bagnato and D. Kleppner, Phys. Rev. A **44**, 7439 (1991).  
 [24] C. P. Chu, M. C. Chang, and Q. Niu, arXiv:0709.1407 (2007).  
 [25] J. Keeling, L. S. Levitov, and P. B. Littlewood, Phys. Rev. Lett. **92**, 176402 (2004).  
 [26] M. Z. Maialle, E. A. de Andrada e Silva, and L. J. Sham, Phys. Rev. B **47**, 15776 (1993).  
 [27] C. J. Pethick and H. Smith, *Bose-Einstein Condensation in Dilute Gases* (Cambridge University Press, Cambridge, 2002), 1st ed.  
 [28] T. Hakioglu and M. Sahin, Phys. Rev. Lett. **98**, 166405 (2007).  
 [29] J. W. Ye, arXiv:0712.0437 (2007).  
 [30] J. Kasprzak *et al.*, Nature **443**, 409 (2006); H. Deng, G. S. Solomon, R. Hey, K. H. Ploog, and Y. Yamamoto, Phys. Rev. Lett. **99**, 126403 (2007); R. Balili, V. Hartwell, D. Snoke, L. Pfeiffer, and K. West, Science **316**, 1007 (2007).